

CONF-820125--1

MASTER

A 0.4 mm INTERFEROMETER SYSTEM USING DIELECTRIC WAVEGUIDE

D. P. Hutchinson, C. H. Ma,
P. A. Staats, and K. L. Vander Sluis

Physics Division, Oak Ridge National Laboratory,*
Oak Ridge, Tennessee 37830 USA

CONF-820125--1

DE82 010197

*Work sponsored by the Division of Magnetic Fusion
Energy, U.S. Department of Energy, under contract
W-7405-eng-26 with the Union Carbide Corporation.

By acceptance of this article, the
publisher or recipient acknowledges
the U.S. Government's right to
retain a nonexclusive, royalty free
license in and to any copyright
covering the article.

DISCLAIMER

This document contains information which is the property of the U.S. Government and is loaned to you. It and its contents are not to be distributed outside your organization. If you are not an authorized recipient, please notify the person to whom this document was loaned. If you are an authorized recipient, you are to use this information only for the purpose for which it was loaned to you. It is not to be used for any other purpose, and it is not to be reproduced, stored in a retrieval system, or transmitted in any form or by any means, electronic, mechanical, photocopying, recording, or by any information storage and retrieval system, without the prior written permission of the U.S. Government.

A 0.4 mm INTERFEROMETER SYSTEM USING DIELECTRIC WAVEGUIDE

D. P. Hutchinson, C. H. Ma,
P. A. Staats, and K. L. Vander Sluis

Physics Division, Oak Ridge National Laboratory*
Oak Ridge, Tennessee 37830 USA

A 0.4 mm submillimeter-wave, phase-modulated polarimeter/ interferometer is used for simultaneous time-dependent measurement of line-averaged electron density and poloidal field-induced Faraday rotation along chords of the plasma column in ISX-B tokamak. Heterodyne detection and hollow dielectric waveguide are utilized to achieve the high sensitivity required for the multichord experiment.

Introduction

The radial distribution of the toroidal plasma current in tokamak is of prime importance for understanding fundamental problems (e.g., transport phenomena, MHD instability, and plasma pressure effects). Various methods for measuring the distribution have been tried (1-12); however, none are used as a routine method. Theoretical analyses have shown that the distribution can be obtained indirectly by measurement of the poloidal magnetic field which can be determined by projecting linearly polarized farinfrared (FIR) laser beams through the plasma and measuring the Faraday rotation of the polarization (13-15). Since the rotation angle of the polarization vector is proportional to the line integral of electron density times the poloidal magnetic field along the path, the electron density profile must also be measured simultaneously in order to unfold the current distribution. During the last decade, the FIR interferometers have been used to reliably measure electron density of tokamak plasmas (16-19). To our knowledge, simultaneous measurement of Faraday rotation and electron line density using submillimeter wave has

*Work sponsored by the Division of Magnetic Fusion Energy, U.S. Department of Energy, under contract W-7405-eng-26 with the Union Carbide Corporation.

been achieved only recently (20). In the combined polarimeter/interferometer, the authors employed a ferrite polarization modulator which was driven by audio frequency current. The detector signal at the modulation frequency was synchronously detected by a high-sensitivity lock-in amplifier. This paper presents the recent results on a modified system.

The modification is the result of two major improvements to the laser and detection systems: (1) use of a hollow dielectric waveguide for laser transport to and from the tokamak and (2) modification of the electronics to allow heterodyne detection of the Faraday rotation signals. The previous optics system utilized open-air transmission of laser beams by a set of relay lenses. The system was subject to considerable loss ($\sim 10^4$ to 10^6) due to water-vapor absorption during humid summer days and lens losses due to Fresnel reflection and material absorption. The use of pressurized dielectric waveguide in the present system has not only greatly reduced the absorption in humid air but has also eliminated the need of focusing elements for laser transport. Sufficient stability is achieved by using the reference interferometer beam as a local oscillator for the superheterodyne receiver system. These improvements have made possible multichord measurements of electron density and Faraday rotation on the TSX-B tokamak.

Theory and Description of the System

A schematic diagram of the polarimeter/interferometer system is shown in Fig. 1. The photon sources are two cw 393 μm ferric acid lasers, optically pumped by CO_2 -waveguide lasers. The FIR cavities are tuned such that the two oscillate at frequencies differing by Δf of the order of 500 kHz. The linearly polarized beam of the source laser is passed through the polarization modulator into the dielectric waveguide and is focused on the center of the plasma chamber. The lasers and the ferrite polarization modulator have been previously described in detail (20,21). The waveguides are made of 2.54-cm ID plexiglass tubing. Water vapor absorption is eliminated by slightly pressurizing the waveguide with dry

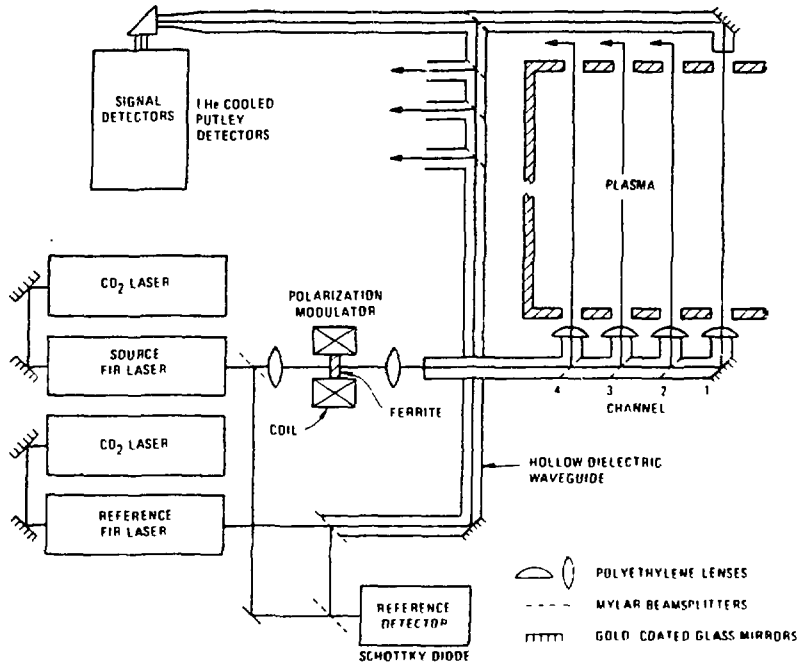


Figure 1. Schematic of the submillimeter-wave polarimeter/interferometer system using hollow dielectric waveguide and heterodyne detection.

nitrogen. Upon entering the waveguide, the submillimeter laser beams assume an EH_{11} high-order waveguide mode and are transmitted without the need for relay lenses to maintain a uniform beam size. Thin transparent pellicles of mylar are used to seal the ends of the waveguide against the atmosphere. For the sake of simplicity, only one of the four chords is shown in Fig. 1 and is henceforth described. As shown in Fig. 2, the probing beam traverses a poloidal plasma cross section and experiences a phase shift, ϕ , (22)

$$\phi(\text{rad}) = 2.82 \cdot 10^{-13} \cdot \lambda \int_{-Z_0}^{+Z_0} n_e(z) dz \quad (1)$$

and a Faraday rotation, θ_p , (14)

$$\theta_p(\text{deg}) = 1.5 \cdot 10^{-12} \cdot \lambda^2 \int_{-Z_0}^{+Z_0} n_e(z) B(z) dz \quad (2)$$

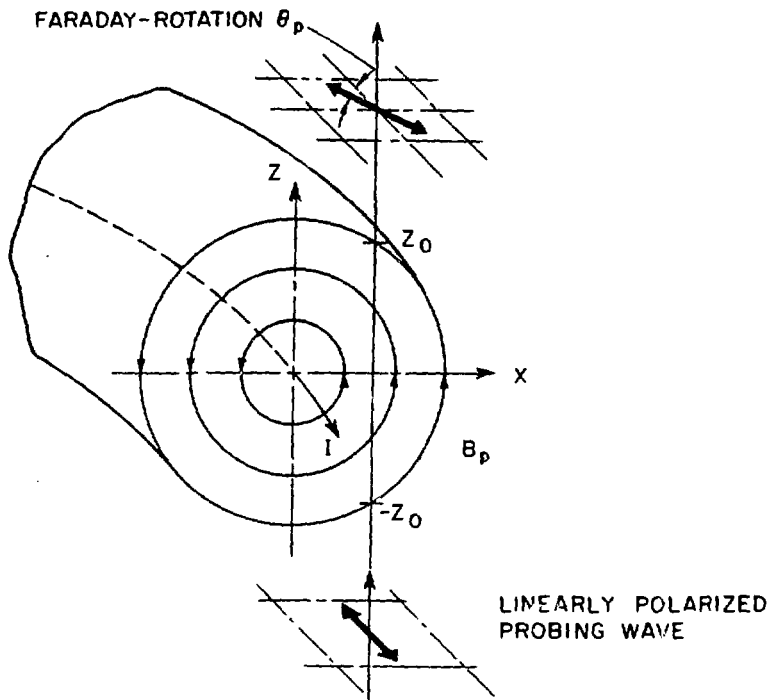


Figure 2. Geometry and coordinate system for plasma in a tokamak.

where λ is the probing wavelength in cm, $n_e(z)$ is the electron density along the chord in cm^{-3} , $B_z(z)$ is the component of B_p along the chord in KG, and $2z_0$ is the length of the chord in cm. Emerging from the chamber, the beam enters again into waveguide and is directed on to a He-cooled Putley detector. Part of the beam from the reference laser is mixed first in a Schottky diode with a portion of the source laser, which is split off before passage through the modulator, and the remainder is guided to the Putley detector to mix with the probing beam. The output of the Schottky diode is a sinusoid at frequency Δf and is used as the reference signal for the phase detection. The output of the Putley detector, V_s , can be expressed by the following relation (23).

$$V_s = \left\{ \sqrt{R_s P_s} \cos[\theta_p + \theta_m \sin(\omega_m t)] \sin[(\omega + \Delta\omega)t + \phi] + \sqrt{R_r P_r} \sin(\omega t) \right\}^2 \quad (3)$$

$$= \sqrt{R_s R_r P_s P_r} \cos[\theta_p + \theta_m \sin(\omega_m t)] \cdot \cos(\Delta\omega t + \phi) + \text{terms of dc and other frequencies,}$$

where R_s and R_r are the responsivity of the signal and reference detector, respectively, θ_m is the amplitude of the modulation angle, ω_m is the modulation frequency, and P_s and P_r are the power of the probing and reference beam at the detector respectively.

The signal processing scheme is shown in Fig. 3. Detector signals are filtered, amplified, and fed into a digital phase detection circuit to extract the phase shift due to plasma density. A square-law detection circuit is utilized to demodulate the phase-modulated signal, and it provides a sinusoidal signal at ω_m whose amplitude is proportional to $R_s R_r P_s P_r J_1(2\theta_m) \sin(2\theta_p)$, where $J_1(2\theta_m)$ is the Bessel function of the first kind with order one. This signal is synchronously detected by a lock-in amplifier, which yields an output voltage,

$$V_{out} = \frac{1}{2} R_s R_r P_s P_r L A J_1(2\theta_m) \sin(2\theta_p) \quad (4)$$

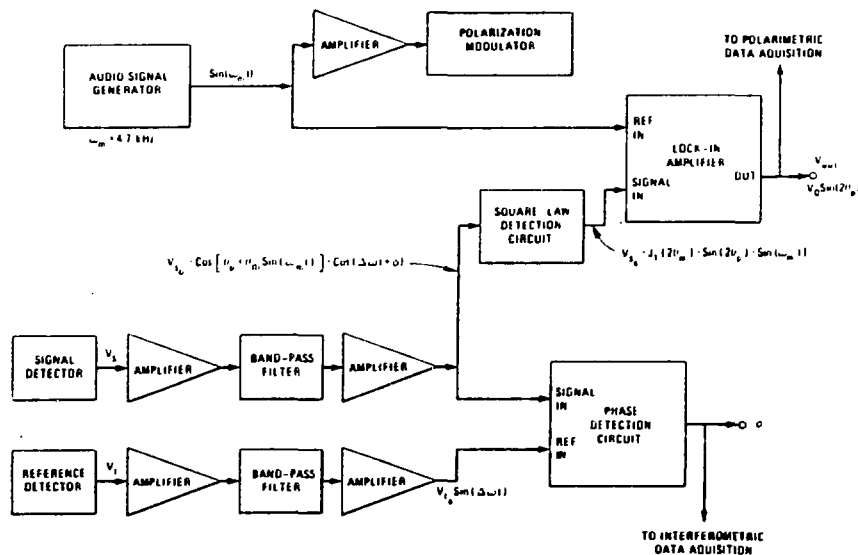


Figure 3. Signal processing scheme of the combined polarimeter/interferometer system.

where L is the loss in the filter and A is the total voltage gain of the amplifiers. The values of the individual components of Eq. (4) may be lumped into a single calibration constant, V_o , so that Eq. (4) becomes

$$V_{out} = V_o \sin(2\theta_p) \quad (5)$$

where $V_o = \frac{1}{2} R_s R_r P_s P_r L A J_1(2\theta_m)$ (in volts). The value of V_o can be obtained by inserting a mechanical 45° polarization rotator (24) in the path of the probing beam and measuring the value of V_{out} without plasma in the chamber. It is interesting to note that V_{out} is a direct measure of small θ_p , since $\sin(2\theta_p) \approx 2\theta_p$, and Eq. 5 becomes

$$\theta_p = V_{out}/2V_o \quad (6)$$

The outputs of the phase detector and the lock-in amplifiers are displayed on oscilloscopes for photographic recording and are digitized for computer storage and processing.

Experimental Results

The polarimeter/interferometer has been routinely employed to study the neutral-beam-heated plasma discharges in ISX-B tokamak for over a year (more than a thousand plasma shots). A data processing code has been developed to reconstruct the line-averaged plasma density from the measured fringes of phase shift almost instantaneously after each discharge. The time resolution of the interferometer, set by the frequency of the beat signal, is typically $2 \mu s$. It can easily be changed by detuning one of the FIR cavities. The standard deviation of the output of the interferometer of a constant phase shift is less than 5×10^{-2} fringe. Since one fringe corresponds to a line density of $1.05 \times 10^{13} \text{ cm}^{-3}$, density variations as small as $5.25 \times 10^{11} \text{ cm}^{-3}$ can be measured. The polarimeter shows a sensitivity of the order of one milliradian and a time resolution of approximately

2 msec. The time evolutions of the line-density, Faraday rotation, and the total plasma current of a typical plasma discharge are shown in Fig. 4. A neutral beam of approximately 1 MW was injected at the time of 80 msec after the beginning of the discharge. As shown in Fig. 4, the density was "clamped" to approximately the same level as it was immediately prior to the injection for ~ 50 msec. Since the Faraday rotation is proportional to the integral of density times the poloidal field, the time variation of Faraday rotation should resemble the density during a period of nearly constant current. This effect is verified by the curves in Fig. 4. Figure 5 demonstrates the fast response of the interferometer. During this plasma discharge, a solid hydrogen pellet was injected into the plasma at the time of approximately 170 msec. The pellet caused a density increase of $\sim 3.3 \times 10^{13} \text{ cm}^{-3}$ in channel 1, and $\sim 1.2 \times 10^{13} \text{ cm}^{-3}$ in channel 3. The detailed density variations during the injection can be seen in the inset of Fig. 5. The photograph shows the output of the phase detection circuit before processing with a time scale of $50 \mu\text{s}/\text{division}$. The abrupt increase of density occurs during a period of approximately $400 \mu\text{s}$. The time delay ($\sim 30 \mu\text{s}$) between two curves indicates that the increase of density follows the pellet as it moves from the

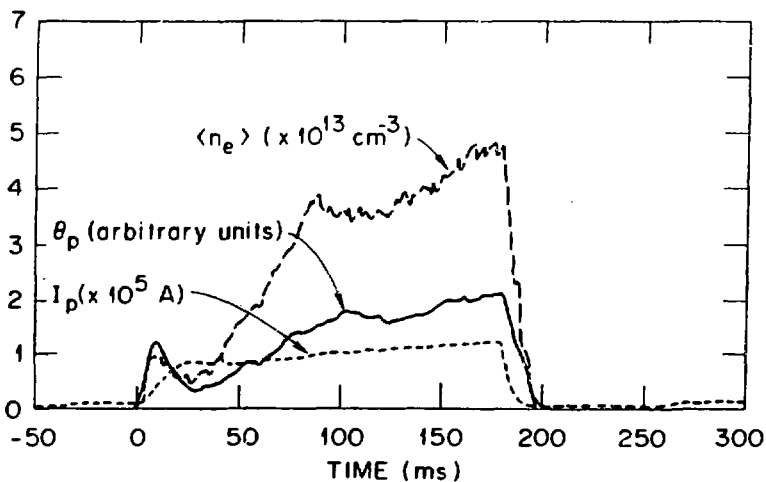


Figure 4. Time variations of Faraday rotation, line-averaged electron density, and total plasma current of ISX-B tokamak.

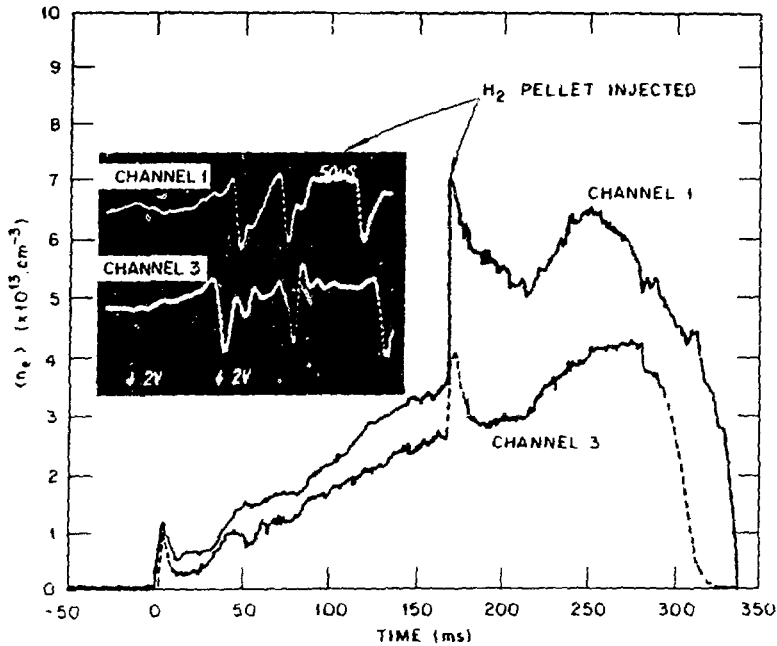


Figure 5. Fast increase of line density is caused by the injection of a solid hydrogen pellet. Inset: output of the phase detector during the injection, time scale 50 ms/division.

outer wall toward the center of the chamber (channel 1). Due to a lack of detectors, the measurement is presently limited to two chords during a single discharge. Typically, during a sequence of ~ 30 identical shots, channel 1 was employed for all shots to monitor the drift of the plasma conditions, and each of the other channels was used for ~ 10 shots. It is found that the reproducibility of plasma is better than 3%. In some cases, the measured parameters during the period of plasma "run down" are not essential for studies of the tokamak plasma in ISX-B. Therefore, in order to increase the speed of data processing, the process of reconstruction is terminated near the end of each shot. Typical display of the line-density variation in four channels is shown in Fig. 6. The position of each channel, relative to the center of the chamber is also indicated in the inset. As shown by the variations of densities in channels 1 and 2, the plasma forms a slightly hollow density profile during the period from ~ 70 msec to ~ 140 msec, and becomes quite flat after the time of 150 msec.

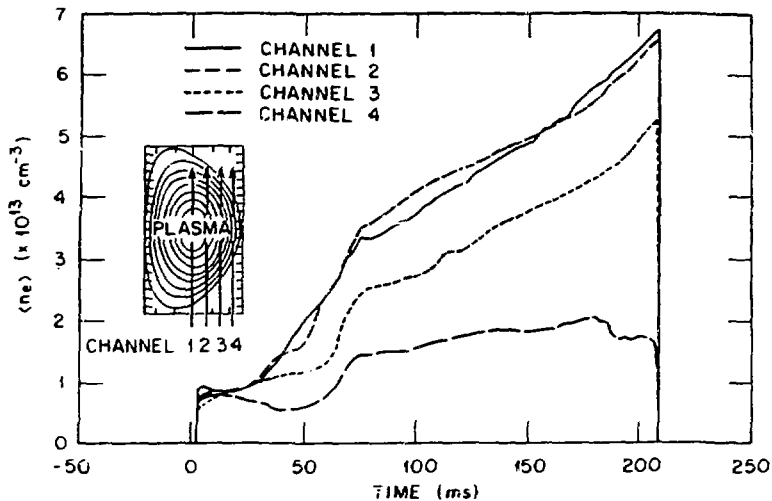


Fig. 6. Typical display of the line-density variations measured by the multichord polarimeter/interferometer system.

Acknowledgments

The authors are greatly indebted to the ISX-B tokamak group for their encouragement, support, and tremendous cooperation. We also wish to particularly thank E. A. Lazarus, M. Murakami, and R. A. Wieland for providing the density profile calculated by the ZORNOC code.

References

1. R. L. Hickock and F. C. Jobes, *Bull. Am. Phys. Soc.* 16, 1231 (1971).
2. A. N. Dellis and J. C. Hosea, Princeton Report MATT 969 (1973).
3. S. Von Gueler, W. Stodiek, and N. Sauthoff, *Phys. Rev. Lett.* 33, 1201 (1974).
4. R. Cano, I. Fidone, and J. C. Hosea, *Phys. Fluids* 18, 1183 (1975).
5. TFR Group, *Proc. 7th Euro. Conf. in Controlled Fusion and Plasma Physics* 1, 11, Lausanne (1975).
6. R. J. Goldston, E. Mazzucato, R. E. Slusher, and C. M. Surko, *Proc. of the 6th IAEA Conf. on Plasma Physics and Controlled Fusion Research, Berchtesgaden* 1, 371 IAEA, Vienna (1977).
7. K. McCormick, N. Kick, and J. Olivain, *Proc. of 8th Euro. Conf. on Controlled Fusion and Plasma Physics* 1, 140, Prague (1977).
8. C. H. Ma, D. P. Hutchinson, and K. L. Vander Sluis, *Bull. Am. Phys. Soc.* 22, 1203 (1977).

9. W. Kunz and G. Dodel, *Plasma Phys.* 20, 171 (1978).
10. W. Kunz, *Nucl. Fusion* 14, 1729 (1978).
11. M. J. Forrest, P. G. Garolan, and N. J. Peacock, *Nature* 271, 718 (1978).
12. C. H. Ma, D. P. Hutchinson, and K. L. Vander Sluis, *Appl. Phys. Lett.* 34, 218 (1979).
13. R. L. Hickok and F. C. Jobes, *Bull. Am. Phys. Soc.* 16, 1231 (1971).
14. F. DeMarco and S. E. Segre, *Plasma Phys.* 14, 245 (1972).
15. A. D. Graig, *Plasma Phys.* 18, 777 (1976).
16. R. W. Peterson and F. C. Jahoda, *Appl. Phys. Lett.* 18, 440 (1971).
17. D. Veron, *Opt. Commun.* 10, 95 (1974).
18. S. M. Wolfe, K. J. Button, J. Waldman, and D. R. Cohn, *Appl. Opt.* 15, 2645 (1976).
19. D. Veron, J. Certain, and J. P. Crenn, *J. Opt. Soc. Am.* 67, 964 (1977).
20. C. H. Ma, D. P. Hutchinson, K. L. Vander Sluis, and P. A. Staats, *Proc. Int. Infrared and Millimeter Waves Conf.*, Miami Beach, Florida, 1979; also *Nucl. Fusion* (submitted 1980).
21. D. P. Hutchinson, P. A. Staats, K. L. Vander Sluis, and J. B. Wilgen, Oak Ridge National Laboratory Report ORNL/TM-7015 (1979).
22. R. A. Alpher and R. A. White, *Plasma Diagnostic Techniques*, ed. R. H. Huddleston and S. L. Leonard (Academic Press, New York, 1965).
23. F. A. Jenkins and H. E. White, *Fundamentals of Optics*, McGraw-Hill, New York, 1950.
24. D. P. Hutchinson, C. H. Ma, P. A. Staats, and K. L. Vander Sluis, *Proc. Conf. on Lasers and Electro-Optics*, Washington, D.C., 1981.